Ion Mobility Measurement by Dc Tomography in an Rf Quadrupole Ion Trap

Wolfgang R. Plass,† Lynn A. Gill, Huy A. Bui, and R. Graham Cooks*

Department of Chemistry, Purdue University, West Lafayette, Indiana 47907-1393

Received: December 10, 1999; In Final Form: March 29, 2000

A nonintrusive tomographic method sensitive to the spatial distribution of trapped ions in the rf quadrupole ion trap is used to investigate ion cooling in the course of collisions with helium. Cooling commences after coherent excitation, by a resonant ac signal, of a mass-selected population of ions and its progress is followed using a short monopolar dc pulse to probe the position of the ion cloud. The amplitude of the probe dc pulse is selected such that it is sufficient to eject ions at some phases and not others. The abundance of the remaining trapped ion population is recorded by a scan of the rf amplitude and thus provides information on the axial secular motion of the original trapped ions. Ions of identical nominal mass, but different chemical composition (krypton, benzene-d_6, and 1-hexene, all nominal mass 84 Da), are studied using pressures chosen to give cooling periods on the order of 10 ms. The maximum excursion in the axial direction, when plotted as a function of cooling time, provides information on the cooling process. The relative cooling times for the ions examined agree with calculated or experimentally known, velocity-dependent collision cross sections. Cooling times, using 0.46 mTorr of helium when operating the ion trap at Mathieu parameter $q_z = 0.278$, were 12 ms for krypton, 9.5 ms for benzene-d_6, and 7 ms for 1-hexene. Simulations of ion motion made using the ion trap simulation program, ITSIM, with ion/neutral elastic collisions enabled, gave results that closely match and augment the experimental data. Methods for increasing the resolution of the experiment are discussed.

Introduction

The rf quadrupole ion trap (Paul trap) is a mass spectrometer that is seeing increasingly widespread use.[1] While it is a small, relatively simple device, the motion of trapped ions is complex and its elucidation is a topic that has attracted a great deal of attention. Various studies on ion motion have been reported based on analytical solutions,[2−6] simulations,[6−12] and experiments.[13−21] The first experiments aimed at characterizing trapped ion motion were those of Wuerker,[13] who photographed charged aluminum particles to follow their trajectories. Twenty years later, Knight and Prior used laser-induced fluorescence to detect atomic ions and determine the size of the trapped ion cloud.[14] Experimental investigations into the motion of ions in the quadrupole ion trap were further refined by the laser photodissociation method, developed jointly by this laboratory and that of Hemberger at Los Alamos National Laboratory.[16,17] In this experiment, ion positions are measured as a function of time by firing a laser across the trap in either the axial or radial direction. Ions in the path of the laser are converted to photofragments, the abundances of which serve to map the temporal and spatial distribution of the parent ions. By exciting the trapped ions into coherent motion or varying the position of the laser beam, spatial distributions and ion cloud velocities can be measured. In 1994 Lammert et al. used a fast dc pulse to translationally excite a population of trapped ions and laser tomography to measure the characteristic frequencies of their axial motion.[18] Laser tomography was subsequently used by Cleven et al. to characterize the spatial distribution and motion of trapped ions as a function of ion population and ion trap geometry, including the ratio of the axial to radial dimensions.[19]

These laser tomography studies provided important insights into the motion of ions in the quadrupole ion trap, especially after coherent excitation which is typically used to cause collisions with the helium bath gas, an essential step in performing tandem mass spectrometry with this instrument.[22−24] Similar information was obtained using the ion trap simulation program, ITSIM, which was being developed simultaneously.[25,26] In spite of the value of the laser tomography studies, they required that slots be machined into either the ring or end-cap electrodes (depending on whether axial or radial tomography was to be performed) to allow laser beam entry to probe the trapped ions. These slots affect the fields experienced by the trapped ions and, among other consequences, are known to cause mass shifts.[19] As an alternative to the use of laser photodissociation to monitor the position of an ion cloud, Weil et al.[21,27] showed that dc tomography could be used to characterize ion motion. In this experiment, the ion population being studied is subjected to a short dipolar or monopolar dc pulse of appropriate amplitude. This ejects some or all the ions from the trap, depending on the phase of their motion and the operating conditions chosen. Hence by repetitively creating an ion population, exciting it using either an ac (in this work) or a dc signal, and then applying a probe dc pulse of appropriate amplitude at varying times after excitation, the periodic motion of the ion cloud can be followed. This is the technique of dc tomography. An advantage of dc tomography over laser tomography to characterize trapped ion motion is that the physical geometry of the electrodes is not modified and hence ion motion is unperturbed until the impulsive ejection event.

Recently, a theory for dc tomography has been developed.[28] In the general case, the amplitude of ion motion after the dc probe pulse depends in a complex fashion on the mass-to-charge ratio of the ions, their characteristic frequencies, the amplitude

* Corresponding author. E-mail: cooks@purdue.edu.

† On leave from II. Physikalisches Institut, Justus-Liebig Universität Giessen, 35392 Giessen, Germany. Work done in partial fulfillment of the requirements of the doctoral degree.

10.1021/jp994356c CCC: $19.00
Published on Web 05/02/2000

and phase of ion motion before the application time of the pulse, the pulse voltage, and the rf phase at the time of application of the pulse. Appropriate choice of the pulse width can almost completely remove the dependence on mass-to-charge ratio, ion frequencies, and rf phase:[28] (i) If the pulse width is chosen to be short compared to the period of the secular oscillation, the oscillation amplitude after the pulse is almost independent of the mass-to-charge ratio and of ion frequency. Hence dc pulse excitation can be used as a broadband excitation method. (ii) The rf phase dependence vanishes for some specific values of the pulse width. A pulse width slightly larger than one rf period fulfills both conditions adequately for most practical purposes, causing the oscillation amplitude after the pulse to depend primarily on the secular ion velocity before the dc probe pulse and the pulse voltage. Tomography data can be obtained by choosing the dc pulse voltage such that ions with a secular velocity of zero are brought close to the end-cap electrodes by the dc pulse. This choice also means that ions with secular velocities parallel to the electric field achieve even larger oscillation amplitudes and either impinge on the end-cap electrodes or are ejected from the trap. Ions with secular velocities which are antiparallel to the electric field acquire smaller oscillation amplitudes and remain trapped. The coherent oscillation of an ion cloud with a finite spread in ion velocities can thus be monitored by measuring the number of ions remaining in the trap after application of the dc probe pulse. Since the spatial and velocity distribution functions for trapped and cooled ion populations are nearly Gaussian,[16,19] the relationship between secular velocity of the coherent ion cloud and number of remaining ions is nonlinear and the range of ion velocities detectable by this method is on the order of the spread of velocities. Larger velocities can be measured by increasing or decreasing the dc pulse voltage and monitoring just the velocity maxima or minima.

Collisional cooling of translationally excited ions in the helium environment of the quadrupole ion trap is the subject of the present investigation. These experiments can be compared to traditional ion mobility experiments[29−31] in which the time taken for ions to pass a fixed distance through a buffer gas under the influence of a constant electric field is measured. Collisions with a nonreactive drift gas (generally N_2 or Ar) reduce the energy gained from the electric field and produce a constant average ion velocity that is directly proportional to the electric field strength, as well as being dependent on the collision cross section of the particular ion.[31] Spatial separation is achieved based on differences in mobility. Ion mobility spectrometry emerged as an analytical technique in the early 1970s, mostly because of its very high sensitivity.[32−34] When the temperature and pressure are held constant, the mobility depends on ion charge, reduced mass, and collision cross section. The collision cross section, determined by the interaction potential between ion and neutral atom or molecule, depends on the geometric size of the ion, among other factors. Ion mobility measurements, especially on mass-selected ions, recently have proved to be an important new source of information on gas-phase ion structures and conformations. These measurements have been particularly valuable in assigning structures to carbon cluster ions[35,36] and to peptides and proteins.[37−39] They have been shown to be a source of dynamical[39] as well as structural information on biological ions. For example, they have provided insights into the process of folding and unfolding of protein ions (not necessarily by routes analogous to those which occur in aqueous solution) as a function of charge state and solution conditions prior to ionization.

The possibility of making mobility measurements, even crudely, in a simple, modified, commercial instrument forms the basis for the present investigation. The quadrupole ion trap operates under conditions where ions are cooled by collisions with a helium buffer gas before mass-selective ejection. This means that elastic scattering cross sections are an important determinant of the details of ion motion in the trap. A significant difference between the quadrupole ion trap and the linear drift tube is that ions in the ion trap do not have a constant velocity because of the alternating electric field. Instead, they move under the influence of a parametric oscillator and large spatial separations due to differences in collision cross section clearly cannot be expected. However, it is shown in this study that the quadrupole ion trap can be used to measure the cooling times for ions of identical mass but different collisional cross sections. These measurements are of interest because of the importance of elastic collisions in controlling ion motion and hence ion trap performance. They are also of interest in that they provide a characteristic, other than mass-to-charge ratio, that serves to distinguish ions in the Paul trap. Because the ions in the ion trap do not have a nearly constant velocity as do ions in traditional ion mobility experiments, calculation of ion mobilities from the measured cooling time is more complicated than from a measured drift time. Numerical modeling is required to compare the results with literature values on ion mobilites or collision cross sections. The latter are of interest for the present work.

In evaluating the experimental results, recourse is had to the ion trap simulation program, ITSIM 5.0.[10,40] This program allows the motion of a collection of ions to be followed. ITSIM includes the effects of nonidealities in the electric field and explicitly considers collisions on a stochastic basis. In a number of recent studies[11,20,41,42] simulations have served as a valuable tool in elucidating and even predicting experimental results. ITSIM is used here to investigate the dc tomography technique and to quantitatively reproduce the experiment under the same operating conditions.

Experimental Section

A previously described[22] prototype ion trap mass spectrometer (ITMS) was used for all experiments. An external rf generator (Hewlett-Packard 33120A 15 MHz Function/Arbitrary Waveform Generator) was utilized to achieve a more stable rf voltage reference than that provided by the internal crystal oscillator. This rf generator was connected to the ITMS electronics via a CMOS interface. A second arbitrary waveform generator, identical to the first, was used to produce an ac excitation signal. The ac signal was connected to one end-cap electrode via an analogue switch and a balun box. To the other end-cap electrode, a dc pulse was applied as needed from a fast high voltage dc pulser (Directed Energy Inc., Ft. Collins, CO). The ITMS instrument has a custom-built board[43] that allows the rf, ac, and dc voltages to be phase-locked.

The scan function used incorporated steps for mass selection, ion cooling, resonance excitation, ion ejection, and trapped residual ion mass analysis using an rf amplitude scan (Figure 1). Ionization was achieved by internal electron ionization for a period of 20 ms at an rf amplitude and frequency corresponding to a value of the Mathieu parameter $q_z = 0.22$. Isolation of the ions of the mass-to-charge ratio of interest was achieved by rf-dc apex isolation.[44] After isolation, the selected ions were given a period of 20 ms to cool to the center of the trap at $q_z = 0.278$. Subsequently, a 250 $mV_{(p-p)}$, 200 μs, 110 kHz ac excitation pulse was used to cause the ions to oscillate coherently at their secular frequency. These oscillations were then mapped

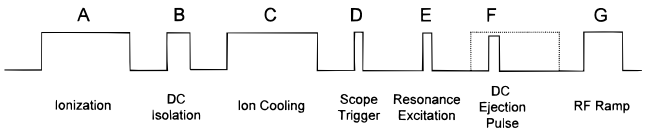

Figure 1. Timing diagram displaying the sequence of events used to cause and then to probe the coherent oscillation of a cloud of mass-selected ions in an ion trap mass spectrometer. The entire experiment is repeated at various delay times between the pump and the probe events in order to acquire the cooling data reported in this paper. (A) Ionization for 20 ms at $q_z = 0.22$. (B) rf−dc apex isolation for 5 ms. (C) Ion cooling for 20 ms at $q_z = 0.278$. (D) Scope trigger. (E) Pump event, 250 $mV_{(p-p)}$ 110 kHz ac resonance excitation for 200 μs. (F) Probe event, 92 V monopolar dc ejection pulse applied for 1.2 μs. (G) Mass-selective instability scan.

using dc tomography.[21] To achieve this, a 92 V, 1.2 μs dc pulse was applied to one end-cap electrode at varying times, starting at 45 μs after the ac excitation pulse. The time of application for the dc pulse was varied using a digital delay generator (Stanford Research Systems DG535). The ions remaining in the ion trap, after the application of the dc pulse, were ejected using a forward rf amplitude scan and detected by the electron multiplier.

Helium was used as the buffer gas for all experiments at a pressure of 0.46 and 0.69 mTorr, measured with a Bayert-Alpert type ionization gauge. All reported pressures are corrected for gauge response.[45] They are lower than the 1 mTorr of helium that is normally used for mass-selective instability scans. The decrease in buffer gas pressure was chosen to increase the cooling time. Note that, although the pressure is given here to two significant digits to allow an accurate relative comparison, its absolute value is subject to a significantly larger uncertainty. Krypton, benzene-d_6, and 1-hexene, each of which gives an abundant ion at m/z 84, were used for these experiments. The corrected analyte pressure was 6×10^{-7} Torr.

To accurately record the secular oscillations of the translationally excited ions moving in the axial direction in the ion trap mass spectrometer, three consecutive secular cycles were examined by dc tomography at a sampling rate of one point every 500 ns. Then three cycles were again recorded but with the delay increased by 1 ms, until the entire cooling curve had been recorded. Ion abundance was measured using the peak height as derived from the amplified electron multiplier output recorded using a digital storage oscilloscope (Tektronix model TDS 540). The oscilloscope was triggered prior to resonance excitation by a digital pulse sent from the ITMS electronics.

Simulations

Simulations of ion motion were carried out using the ion trap simulation program ITSIM 5.0.[40] The program is designed to calculate the trajectories of a large number of ions to obtain qualitative and quantitative information about phenomena connected with ion motion in rf ion traps. At the beginning of the simulation, the ions (typically in numbers from 1 to 10^4) are created with user-definable physical and chemical properties and initial positions and velocities described by various distribution functions. In ITSIM trajectories are calculated using a standard fourth-order Runge−Kutta method or fifth- or eighth-order Runge−Kutta methods with error control and adaptive step size. The electric field is determined either from a multipole expansion or by field interpolation from an array of precalculated electric potential values.[11] For the particular simulations presented here, the fourth-order Runge−Kutta method with a fixed stepsize of 10 ns and the multipole expansion method with expansion coefficients[28] appropriate for an Finnigan ITMS with stretched electrode configuration was used. During the simulation, ion motion can be displayed using various display modes.[10] In addition, the trajectory data can be stored in memory or processed while the simulation is running. In this way, oscillation amplitudes and average kinetic energies can be calculated for large sets of ions. Ions that leave the trapping volume may hit the electrodes or a detector positioned behind the exit end-cap electrode. According to the conditions during ion ejection or at the end of the simulation, mass spectra and information about the distribution of ion position, energy, collision count, and phase relationships can be displayed. All data can be saved or exported to other application programs.

The collision model used for these simulations determines when a collision occurs between an ion and a buffer gas atom from the collision probability

$$P(v_r) = \sigma(v_r) \cdot v_r \frac{p}{kT} \, dt \qquad (1)$$

where v_r is the relative velocity between ion and neutral buffer gas target, $\sigma(v_r)$ is the velocity-dependent collision cross section, p and T are the buffer gas pressure and temperature, respectively, k is Boltzmann's constant, and dt is the time interval considered. At each time step, a buffer gas atom is assigned a random velocity from a Maxwell−Boltzmann distribution corresponding to the buffer gas temperature. The collision probability for the time step interval is calculated and compared with a random number generated from a uniform distribution. If a collision occurs, the change in the ion's velocity is determined using a random scattering angle from an isotropic distribution of scattering angles in the center-of-mass frame and assuming an elastic collision process.

The assumption of isotropic scattering angles applies for the classical scattering of smooth elastic spheres,[46] but not necessarily for ions with complex structures. Calculations and experiments indicate that the differential collision cross section is much larger for small scattering angles than is consistent with the assumption of isotropic scattering.[46] However, since collisions with small scattering angles do not contribute significantly to the average momentum transfer, underestimation of the forward scattering does not seriously influence ion mobility calculations. Moreover, it is advantageous to assume isotropic scattering in the center-of-mass frame, since in that case the total elastic scattering cross section and the momentum transfer cross section are equal.[46] This allows the use of momentum transfer cross sections for determination of the collision probability rather than elastic scattering cross sections; one still obtains the correct average momentum transfer, which primarily determines the effects of collisions of ions in a light buffer gas in the rf ion trap. Experimental momentum transfer cross sections for a much larger range of compounds, target gases, and collision energies are available[47−51] than would be for the case of elastic scattering cross sections.

In traditional drift-tube ion mobility experiments, the velocity dependence of the collision cross section often can be ignored. However, recently it has been observed that a change in buffer gas temperature results in drastically different collision cross sections, even for large polyatomic ions.[52−54] Since ions in the rf ion trap constantly change their velocity, velocity-dependent cross sections have been used here. For krypton, momentum transfer cross sections in a helium buffer gas obtained in traditional ion mobility experiments by Johnsen and Biondi[55,49] were used as collision cross sections. For benzene-d_6 and 1-hexene ions in helium buffer gas, collision cross sections for the energy range of interest were not available. They were

TABLE 1: Cooling Times for Different Ions of *m/z* 84

analyte	collision cross section (Å²)[a]	helium buffer gas press. (mTorr)	cooling time (ms)[b] expt	simuln
krypton	28.6	0.46	12	13
benzene-d_6	53.9	0.46	9.5	9
1-hexene	66.6	0.46	7	7
krypton	28.6	0.69	8	*c*

[a] Derived from the literature for a collision energy in the center-of-mass frame of 0.04 eV, see text. [b] Time required for the signal amplitude to decreases below 5% of its initial value. [c] Value was not obtained.

obtained by calculation. Following an approach developed by Bowers et al.,[54] the cross sections for the collision of the helium buffer gas atom with either a hydrogen or carbon atom of the molecular ion were taken from the literature assuming a (12, 6, 4) potential[31] and using Lennard-Jones parameters reported by Bowers et al.[54] Then, the total cross section of the ion was calculated[56,57] as an orientationally averaged projection cross section, assuming hard sphere interactions between each atom of the ion and the buffer gas atom. While this method for calculating collision cross sections has been shown to be less accurate than rigorous trajectory calculations using the entire ion−atom potential,[39,58] it was chosen for its simplicity. Values for the behavior of the collision cross sections of benzene-d_6 and 1-hexene for large relative velocities were taken from experimental studies of Ring et al.[59] and van Houte et al.[60] After the collision cross section values had been obtained for various relative velocities, they were parametrized for each ion species in terms of the relative velocity v_r by fitting them to a function of the form

$$\sigma(v_r) = c_0 + \frac{c_{1/4}}{v_r^{1/4}} + \frac{c_{1/2}}{v_r^{1/2}} + \frac{c_1}{v_r} \qquad (2)$$

The collision cross sections evaluated from these functions for a collision energy in the center-of-mass frame of 0.04 eV are given in Table 1.

In the simulations performed here, 1000 ions were generated with positions chosen randomly from a Gaussian distribution with a fwhm of 0.7 mm in the axial and 1.2 mm in the radial dimensions and given 10 ms to achieve an equilibrium distribution at $q_z = 0.278$. The initial distribution widths were equilibrium values obtained from preliminary simulations and are consistent with experimentally determined values,[16,19] if the somewhat different ion mass is taken into account. Subsequently, the ions were subject to ac resonance excitation fields and dc pulses using equivalent parameters to those used in the experiment. After application of the dc pulse, the ion motion was calculated for an additional period of 1 ms to determine how many ions remained in stable trajectories. The signal intensity for the simulation was calculated from the square root of the ratio of the number of remaining ions to the original number of ions. This was done since, provided the peak shape in the experiment does not change significantly with ion number, the peak area can be expected to scale with number of ions in the peak, and the peak height with the square root of the number of ions.

Results and Discussion

Preliminary experiments were carried out to optimize the amplitude of the dc pulse used to probe the position of the excited ion cloud. The voltage of this probe pulse was chosen so that after the ions had cooled completely to the center of the ion trap (20 ms after excitation) application of the dc pulse reduced the ion signal to approximately one-half of its original value. The results of a typical experiment, showing the effect of the delay time between resonance excitation and application of the dc probe pulse on the measured intensity of an ion population are shown in Figure 2. Note the characteristic secular oscillations, which in this experiment have a frequency of 110 kHz ($q_z = 0.278$). Data points were acquired at 500 ns intervals, so that 18 data points were taken for each secular cycle. Three cycles were recorded in this way, using increments of 500 ns to investigate the quality of measurement of the individual secular oscillations.

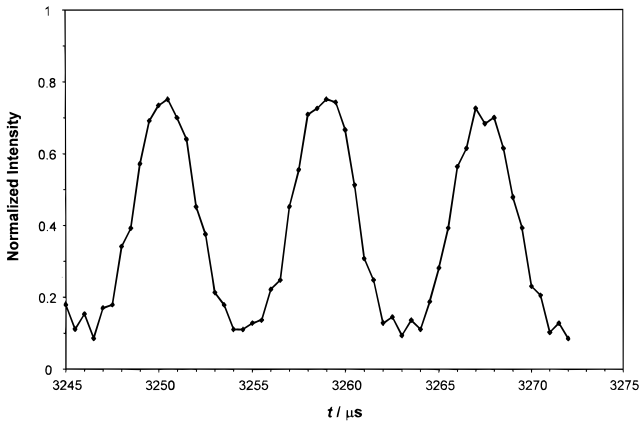

Figure 2. Secular oscillations of a population of krypton ions (*m/z* 84) moving in the ion trap mass spectrometer at $q_z = 0.278$ as determined by the dc tomography experiment. The signal due to the ions remaining trapped after the dc pulse is shown as a function of the application time of the dc pulse. The time $t = 0$ marks the start of the resonance excitation. The helium pressure was 0.46 mTorr.

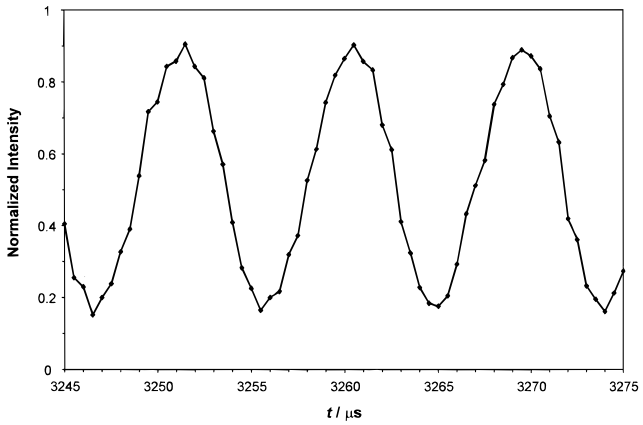

Figure 3. Simulation of the signal due to the ions remaining trapped after the dc pulse as a function of the application time of the dc pulse. The simulation conditions were chosen to match the experimental conditions used to acquire the data shown in Figure 2.

Figure 3 shows the corresponding simulation data recorded using the collision cross section obtained as derived in the previous section and given in Table 1. Apart from a small shift in average intensity, which could be due to the difficulty of accurately determining the maximum intensity of trapped ions in the experiment, and to small differences in the actual and simulated geometries and voltages, the agreement is satisfactory and gives confidence in the quality of the experimental data.

After recording three secular oscillations, the delay time was increased by 1 ms and then again by 54 increments of 500 ns each to record the next three cycles. This procedure was repeated multiple times and used to minimize the total time taken for

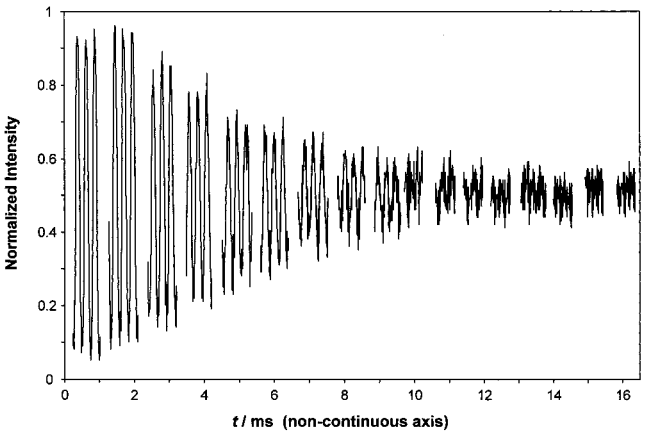

Figure 4. Temporal dependence of the secular oscillations of a population of 1-hexene ions moving in the ion trap mass spectrometer at $q_z = 0.278$ as determined by the dc tomography experiment. The time $t = 0$ marks the start of the resonance excitation.The corrected helium pressure is 0.46 mTorr. Note that the individual segments are shown on a greatly expanded time axis in order to show the individual secular oscillations as well as the long-term time dependence.

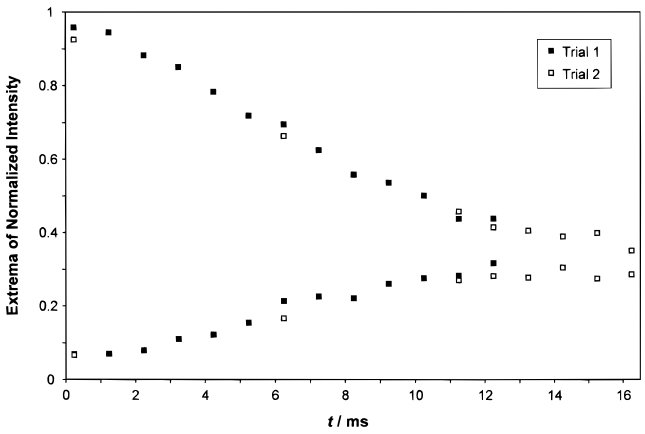

Figure 5. Average of the maxima and the average of the minima of the three secular oscillations at $q_z = 0.278$ at each time step for krypton ions during cooling as a function of the application time of the probe dc pulse. The time $t = 0$ marks the start of the resonance excitation. The corrected helium pressure was 0.46 mTorr. Trial 1 and trial 2 were separated by a few weeks to show the reproducibility of the experiment.

the experiment. Typical experimental results are shown in Figure 4 for 1-hexene. Note that even with this procedure, the data shown required about 10 h to acquire for each ionic species and, during this time, conditions of ion production and helium gas pressure had to be kept constant. As a check that this was the case, the 1 ms steps were not taken sequentially, but in a random fashion. The groups of secular oscillations were collected in the order 245, 16 245, 8245, 4245, 12 245, 14 245, 2245, 10 245, 6245, 15 245, 9245, 13 245, 11 245, 1245, 7245, 3245, and 5245 μs delays. This procedure allowed any systematic errors, such as a change in pressure, to be detected and corrected for, although, in fact, no such correction was necessary. Note that the three-cycle data sets shown in Figure 4 are shown on a greatly expanded scale relative to the overall delay period which is indicated on the abscissa. It is evident from this data that the oscillations of the ion cloud become damped with cooling time.

Figure 5 shows the average of the maxima and the average of the minima of the three secular oscillations at each major time increment for krypton. The reproducibility of this experiment is reflected in the data shown in Figure 5 where trial 1 and trial 2 measurements were separated by a few weeks.

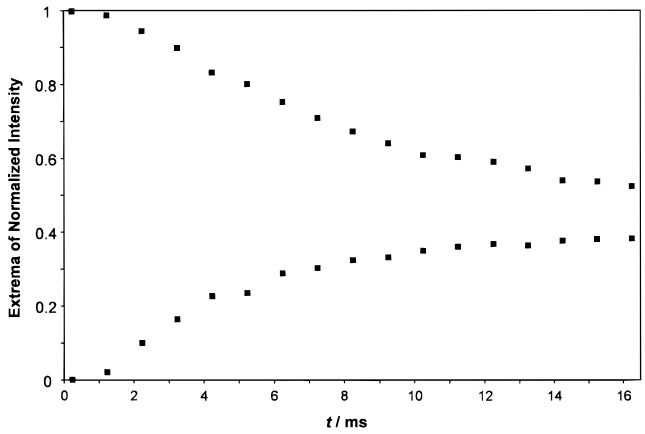

Figure 6. Simulation of the intensity extrema averages of three secular cycles for krypton ions as a function of the application time of the dc pulse. The simulation conditions were chosen to match the experimental conditions used to acquire the data shown in Figure 5.

The results of the corresponding simulation are given in Figure 6. The rate of damping in experiment and simulation is very similar. Further investigation of the cooling process by simulations shows that the damping in intensity is due to two factors: (i) the oscillation amplitude of each individual ion is reduced in collisions by momentum transfer to the buffer gas atoms and (ii) the ion cloud loses its coherence because of the stochastic nature of the scattering process. While the former factor dominates in the early stages of the damping process, it is the latter factor which finally brings the center of the ion cloud to rest in the trap center, although each ion individually, due to the thermal energy of the buffer gas, retains a finite oscillation amplitude.

A striking observation is that the maxima and minima of the signal intensity do not converge to the same value. This is due to the rf phase dependence of the dc pulse excitation process, which is investigated in detail in a separate publication.[28] To correct for this effect, all further plots are renormalized and show only the difference between maxima and minima, reduced by the equilibrium value. The unit intensity value corresponds to the maximum ion signal observed over the total experiment for each analyte, and the value of zero to that of the equilibrium ion signal.

The fact that the average signal intensity converges to about 30% in the experiment, but about 50% in the simulation, could be explained by small differences in the effective dc pulse voltage, width, or pulse form, which determine how many ions are ejected from the trap. Furthermore, the effect of the endcap holes on the electric field inside the trap was neglected in these simulations. The factor decreases the field strength close to the electrodes and lead to ejection of the ions at somewhat lower dc pulse voltages.[28]

The helium pressure dependence of the cooling time was investigated by systematically changing the helium buffer gas pressure. In the case of krypton, the experiment was performed on two separate occasions, first with a helium pressure of 0.46 mTorr and second with a pressure of 0.69 mTorr. Both pressures are corrected values. It can be seen from the data shown in Figure 7 that there is a significant difference in the cooling times using the two bath gas pressures. The cooling time for 0.69 mTorr is shorter by a factor of about $^2/_3$ compared to 0.46 mTorr. To a good approximation, the cooling time should be inversely proportional to the number of collisions and hence the buffer gas pressure. Thus, the result agrees well with the pressure difference of a factor of $^3/_2$.

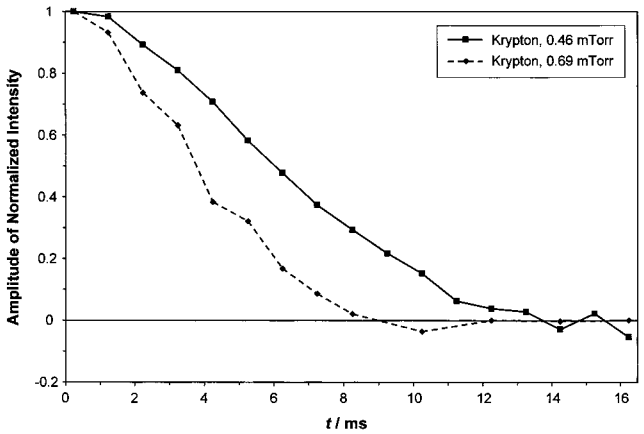

Figure 7. Effect of changing the helium buffer gas pressure by a known amount, on the cooling of ions moving in the quadrupole ion trap. Krypton (*m*/*z* 84) was the analyte at a corrected pressure of 6×10^{-7} Torr and a working point of $q_z = 0.278$.

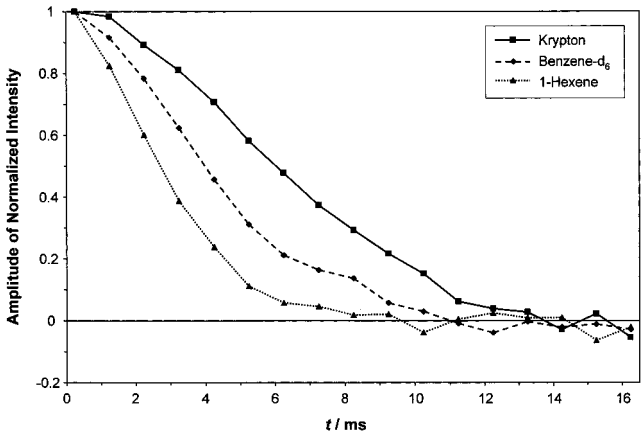

Figure 8. Experimentally determined cooling curves for *m*/*z* 84 ions derived from krypton, benzene-d_6 and 1-hexene. The amplitude of the normalized signal intensity is shown as a function of the application time of the dc pulse used to probe ion motion. The time $t = 0$ marks the start of the resonance excitation. The ions were held at a working point of $q_z = 0.278$ and the helium buffer gas pressure was 0.46 mTorr.

The key experiment is the determination of whether ions with different cross sections cool at different rates, as expected. To investigate this point, krypton, benzene-d_6, and 1-hexene at a helium pressure of 0.46 mTorr were examined. Each of these species yields an ion of *m*/*z* 84, and from traditional ion mobility experiments and theoretical calculations it is known that these ions have different collision cross sections (vide supra). Figure 8 presents ion mobility spectra for krypton, benzene-d_6, and 1-hexene. The cooling curve for krypton is noticeably longer than that for either benzene-d_6 or 1-hexene. These data are presented in tabular form in Table 1 with each cooling time being compared with the calculated collision cross sections at a collision energy in the center-of-mass frame of 0.04 eV. Here, the cooling time is defined arbitrarily as the time taken for the amplitude to decrease to below 5% of its initial value. The values were determined from a polynomial fit to the data. Although the number of data points is limited, the relative cooling times decrease with increasing cross sections, as expected.

A more detailed comparison can be made with the results of simulations, which are displayed in Figure 9. The cooling curves for experiment and simulation are very similar. The cooling times for all three compounds, which are given for simulation and experiment in Table 1, agree well within the uncertainty of the pressure measurement and the collision cross section

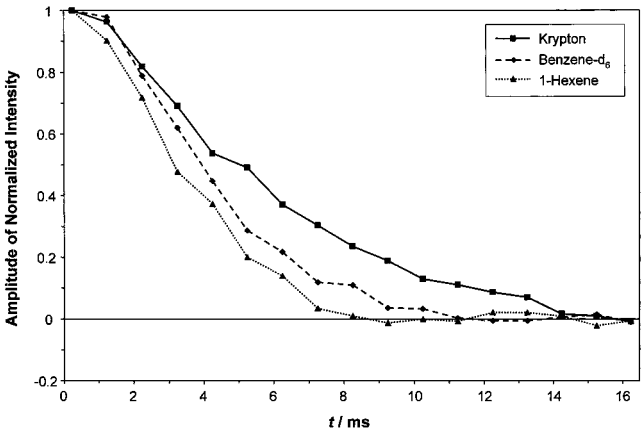

Figure 9. Simulation of cooling curves for *m*/*z* 84 ions derived from krypton, benzene-d_6 and 1-hexene. The amplitude of the normalized signal intensity is shown as a function of the application time of the dc pulse used to probe ion motion. The simulation conditions were chosen to match the experimental conditions used to acquire the data shown in Figure 8.

calculation. However, the initial cooling rate is different between experiment and simulation. The reason for this is currently not understood. Differences in intial conditions, such as the size of the cooled ion cloud, and the neglect of space charge effects in the simulations, might play a role. Collisions between the analyte ions and their neutrals were not taken into account in the simulation; these collisions, while rare, can be expected to be especially effective in causing energy loss, both through elastic collisions and by the charge exchange route.

The excitation time chosen for resonance excitation, and hence the degree of translational excitation, was relatively small. Simulations show that even directly after resonance excitation, the oscillation amplitude of the coherent motion of the ion cloud was about 1.2 mm, which is small compared to the distance of 7.83 mm between trap center and either end-cap electrode. Dc tomography can only be used to observe ion oscillations accurately over a limited range, which is of the order of the width of the ion cloud.[28] Larger oscillation amplitudes would mean larger ion velocities, which would lead to a better resolution of the ion mobility experiment. However, there are three reasons why this is difficult: (i) the motion of the ion cloud would then have to be observed at different positions, viz., with different dc pulse voltages; (ii) inelastic collisions could no longer be ignored for certain analytes; and (iii) the effects of nonlinear field contributions would no longer be negligible.

Conclusions

Dc tomography is a nonintrusive method for the investigation of ion motion in the quadrupole ion trap. The technique can be used to observe the helium collisional cooling of ions in the quadrupole ion trap. The pump/probe technique used here employs resonance excitation of the trapped ion cloud followed by a fast dc pulse to examine the resulting ion motion. The cooling behavior of the *m*/*z* 84 ions formed from krypton, benzene-d_6, and 1-hexene, which are known from traditional ion mobility experiments and calculations to have differing collision cross sections, was found to be characteristically different. A good correlation was shown between the cooling curves for the ions determined experimentally by dc tomography and those found by simulations which use the collision cross sections obtained by traditional ion mobility experiments and calculations. However, the precision of the experiment is not

high, and this offsets the convenience of being able to make the valuable ion mobility measurement using a modified commercial instrument.

More precise results might be obtained by exciting the ion cloud to larger oscillation amplitudes and carefully monitoring the ion oscillation using different dc pulse voltages. In this way, the nonlinear relationship between oscillation amplitude and ion signal could be removed. Dipolar dc pulses could be used instead of monopolar dc pulses to further reduce the rf phase dependence of the signal.[28] Furthermore, dc pulses could be used instead of resonance excitation to achieve coherent ion motion. The dc pulse excitation process is very fast; it is hence independent of collisions which otherwise could occur during the excitation.

Acknowledgment. This project was supported by the Divisions of Chemical Sciences, Office of Basic Energy Sciences, Office of Energy Research, U.S. Department of Energy, and by ThermoQuest Corp. through the Purdue Industrials Association Program. The authors thank Anne Counterman and David E. Clemmer for the projection cross section calculations and Carsten Weil, J. Mitchell Wells, and David E. Clemmer for helpful discussions.

References and Notes

(1) March, R. *J. Mass Spectrom.* **1997**, *32*, 351−369.
(2) Fischer, E. *Z. Phys.* **1959**, *156*, 1−26.
(3) Dehmelt, H. G. *Adv. Atom. Mol. Phys.* **1967**, *3*, 53−72.
(4) Blatt, R.; Zoller, P.; Holzmüller, G.; Siemers, I. *Z. Phys. D* **1996**, *4*, 121−126.
(5) Moriwaki, Y.; Tachikawa, M.; Maeno, Y.; Shimizu, T. *Jpn. J. Appl. Phys.* **1992**, *31*, L 1640−1643.
(6) Franzen, J.; Gabling, R. H.; Schubert, M.; Wang, Y. Nonlinear Ion Traps. In *Practical Aspects of Ion Trap Mass Spectrometry*; March, R. E., Todd, J. F. J., Eds.; CRC Press: Boca Raton, FL, 1995; Vol. 1, pp 49−167.
(7) *Quadrupole Mass Spectrometry and Its Applications*; Dawson, P. H., Ed.; Elsevier Scientific Publishing Co.: New York, 1976.
(8) Alili, A.; Andre, J.; Vedel, F. *Phys. Scr.* **1988**, *T22*, 325−328.
(9) Julian, R. K.; Cooks, R. G.; March, R. E.; Londry, F. A. Ion Trajectory Simulations. In *Practical Aspects of Ion Trap Mass Spectrometry*; March, R. E., Todd, J. F. J., Eds.; CRC Press: Boca Raton, FL, 1995; Vol. 1, pp 221−297.
(10) Bui, H. A.; Cooks, R. G. *J. Mass Spectrom.* **1998**, *33*, 297−304.
(11) Wells, J. M.; Plass, W. R.; Patterson, G. E.; Ouyang, Z.; Badman, E. R.; Cooks, R. G. *Anal. Chem.* **1999**, *71*, 3405−3415.
(12) Quarmby, S. T.; Yost, R. A. *Int. J. Mass Spectrom.* **1999**, *190/191*, 81−102.
(13) Wuerker, R. F.; Shelton, H.; Langmuir, R. V. *J. Appl. Phys.* **1959**, *30*, 342.
(14) Knight, R. D.; Prior, M. H. *J. Appl. Phys.* **1979**, *50*, 3044.
(15) Siemers, I.; Blatt, R.; Sauter, T.; Neuhauser, W. *Phys. Scr.* **1988**, *T22*, 240−242.
(16) Hemberger, P. H.; Nogar, N. S.; Williams, J. D.; Cooks, R. G.; Syka, J. E. P. *Chem. Phys. Lett.* **1992**, *191*, 405−410.
(17) Williams, J. D.; Cooks, R. G.; Syka, J. E. P.; Hemberger, P. H.; Nogar, N. S. *J. Am. Soc. Mass Spectrom.* **1993**, *4*, 792.
(18) Lammert, S. A.; Cleven, C. D.; Cooks, R. G. *J. Am. Soc. Mass Spectrom.* **1994**, *5*, 29.
(19) Cleven, C. D.; Cooks, R. G.; Garrett, A. W.; Nogar, N. S.; Hemberger, P. H. *J. Phys. Chem.* **1996**, *100*, 40−46.
(20) Cleven, C. D.; Nappi, M.; Cooks, R. G.; Garrett, A. W.; Nogar, N. S.; Hemberger, P. H. *J. Phys. Chem.* **1996**, *100*, 5205−5209.
(21) Weil, C.; Wells, J. M.; Wollnik, H.; Cooks, R. G. *Int. J. Mass Spectrom.* **2000**, *194*, 225.
(22) Louris, J. N.; Cooks, R. G.; Syka, J. E. P.; Kelley, P. E.; Stafford, G. C.; Todd, J. F. J. *Anal. Chem.* **1987**, *59*, 1677−1685.
(23) Johnson, J. V.; Yost, R. A.; Kelley, P. E.; Bradford, D. C. *Anal. Chem.* **1990**, *62*, 2162.
(24) McLuckey, S. A.; Glish, G. L.; VanBerkel, G. J. *Int. J. Mass Spectrom. Ion Processes* **1991**, *106*, 213−235.
(25) Reiser, H.-P.; Julian, R. K.; Cooks, R. G. *Int. J. Mass Spectrom. Ion Processes* **1992**, *121*, 49.
(26) Julian, R. K.; Reiser, H. P.; Cooks, R. G. *Int. J. Mass Spectrom. Ion Processes* **1993**, *123*, 85.
(27) Weil, C. Ph.D. Thesis, Justus-Liebig Universität Giessen, 1997.
(28) Plass, W. R. *Int. J. Mass Spectrom.*, in press.
(29) Hill, H. H.; Siems, W. F.; St. Louis, R. H. *Anal. Chem.* **1990**, *62*, 1201A-1209A.
(30) Eiceman, G. A.; Karpas, Z. *Ion mobility spectrometry*; CRC Press: Boca Raton, FL, 1994.
(31) Mason, E. A.; McDaniel, E. W. *Transport Properties of Ions in Gases*; John Wiley & Sons: New York, 1988.
(32) Griffin, G. W.; Dzidic, I.; Carrol, D. I.; Stillwell, R. N.; Horning, E. C. *Anal. Chem.* **1973**, *45*, 1204−1209.
(33) Karasek, F. W.; Kane, D. M. *J. Chromatogr. Sci.* **1972**, *10*, 673−677.
(34) Shumate, C.; St. Louis, R. H.; Hill, H. H. *J. Chromatogr.* **1986**, *373*, 141−173.
(35) Bowers, M. T.; Kemper, P. R.; von Helden, G.; van Koppen, P. A. M. *Science* **1993**, *260*, 1446.
(36) Bowers, M. T. *Acc. Chem. Res.* **1994**, *27*, 324−332.
(37) Wyttenbach, T.; von Helden, G.; Bowers, M. T. *J. Am. Chem. Soc.* **1996**, *118*, 8355−8364.
(38) Valentine, S. J.; Anderson, J. G.; Ellington, A. D.; Clemmer, D. E. *J. Phys. Chem. B* **1997**, *101*, 3891−3900.
(39) Clemmer, D. E.; Jarrold, M. F. *J. Mass Spectrom.* **1997**, *32*, 577−592.
(40) Plass, W. R.; Cooks, R. G.; Goeringer, D. E.; McLuckey, S. A.; Proceedings of the 47th ASMS Conference on Mass Spectrometry and Allied Topics, 1999, Dallas, TX, June 13−18.
(41) Cooks, R. G.; Cleven, C. D.; Horn, L. A.; Nappi, M.; Weil, C.; Soni, M. H.; Julian, R. K. *Int. J. Mass Spectrom. Ion Processes* **1995**, *146/147*, 147−163.
(42) Badman, E. R.; Johnson, R. C.; Plass, W. R.; Cooks, R. G. *Anal. Chem.* **1998**, *70*, 4896−4901.
(43) Lammert, S. A. Ph.D. Thesis, Purdue University, 1992.
(44) March, R. E.; Hughes, R. J. *Quadrupole Storage Mass Spectrometry*; John Wiley and Sons: New York, 1989.
(45) Summers, R. L. NASA Technical Note TN D-5285, National Aeronautics and Space Administration, Washington, DC, June 1969.
(46) McDaniel, E. W. *Collision Phenomena in Ionized Gases*; John Wiley & Sons: New York, 1964.
(47) Ellis, H. W.; Pai, R. Y.; McDaniel, E. W.; Mason, E. A.; Viehland, L. A. *At. Data Nucl. Data Tables* **1976**, *17*, 177−210.
(48) Ellis, H. W.; McDaniel, E. W.; Albritton, D. L.; Viehland, L. A.; Lin, S. L.; Mason, E. A. *At. Data Nucl. Data Tables* **1978**, *22*, 179−217.
(49) Ellis, H. W.; Thackston, M. G.; McDaniel, E. W.; Mason, E. A. *Atomic Data Nucl. Data Tables* **1984**, *31*, 113−151.
(50) Viehland, L. A.; Mason, E. A. *At. Data Nucl. Data Tables* **1995**, *60*, 37−95.
(51) Valentine, S. J.; Counterman, A. E.; Clemmer, D. E. *J. Am. Soc. Mass Spectrom.* **1999**, *10*, 1188−1211.
(52) Mesleh, M. F.; Hunter, J. M.; Shvartsburg, A. A.; Schatz, G. C.; Jarrold, M. F. *J. Phys. Chem.* **1996**, *100*, 16082−16086.
(53) Mesleh, M. F.; Hunter, J. M.; Shvartsburg, A. A.; Schatz, G. C.; Jarrold, M. F. *J. Phys. Chem. A* **1997**, *101*, 968.
(54) Wyttenbach, T.; von Helden, G.; Batka, J. J.; Carlat, D.; Bowers, M. T. *J. Am. Soc. Mass Spectrom.* **1997**, *8*, 275−282.
(55) Johnsen, R.; Biondi, M. A. *Phys. Rev. A* **1979**, *20*, 221−223.
(56) Clemmer, D. E. Personal communication, March 1999.
(57) Henderson, S. C.; Li, J.; Counterman, A. E.; Clemmer, D. E. *J. Phys. Chem. B* **1999**, *103*, 8780−8785.
(58) Shvartsburg, A. A.; Schatz, G. C.; Jarrold, M. F. *J. Chem. Phys.* **1998**, *108*, 2416−2423.
(59) Ring, S.; Naaman, R.; Rudich, Y. *Anal. Chem.* **1999**, *71*, 648−651.
(60) van Houte, J. J.; de Koster, C. G.; van Thuijl, J. *Int. J. Mass Spectrom. Ion Processes* **1992**, *115*, 173−183.